Article

https://doi.org/10.31489/2959-0663/4-23-8

Mariya N. Grigor'eva [iD], Sergey A. Stelmakh[*] [iD]

Baikal Institute of Nature Management SB RAS, Ulan-Ude, Russia;
(*Corresponding author's e-mail: s_stelmakh@bk.ru)

Doped Proton-Conducting Membranes
Based on Heat-Resistant Heterochain Polymers

Fuel cells with solid polymer electrolytes are the most popular chemical current sources and versatile sources of energy today. Proton-conducting membranes based on a guanidine-containing polymer of the cationic type on a polybenzimidazole matrix were obtained in this work. The membranes were created by doping film materials with orthophosphoric acid from a polymer-polymer mixture of N-phenyl-substituted polyhexamethylene guanidine (10%) and polybenzimidazole. In this case, phosphoric acid remains in the membrane due to hydrogen bonds with the functional groups of the polymer and electrostatic interactions resulting from the doping of polyguanidine, which transforms into a polycationic form. As the content of polyguanidine increases in the polymer-polymeric mixture, the proton conductivity of the membrane increases. It was discovered that these membranes possess high thermal stability, with only a 20% mass loss occurring at 350°C. Additionally, they exhibit high proton conductivity of $0.3 \cdot 10^{-1}$ mS/cm at temperatures of 130°C and higher, as well as satisfactory mechanical properties, with a tensile strength (σp) of 21-27 MPa and elongation at break (εp) of 7-11%. The value of activation energy (E_a) is also low, at 0.145 eV, which suggests that these membranes have potential for using them in solid polymer electrolyte fuel cells.

Keywords: polymer films, polymer mixtures, proton-conducting membrane, polyguanidines, polybenzimidazoles, polycationic form, orthophosphoric acid, activation energy.

Introduction

Currently, a large number of proton-conducting membranes (PCM), including sulfonated aromatic polymer membranes, composite polymer-inorganic membranes, polymer-polymer mixture (PPM) membranes, and acid-base PCMs have been developed [1–3]. The main challenge in operating most of these membranes is maintaining satisfactory performance characteristics within the working temperature range of solid polymer electrolyte fuel cells (SPEFC) (100–200 °C) [4, 5]. Acid-base membranes, particularly phosphoric acid-doped polybenzimidazole (PBI) membranes, are of interest due to their potential for high performance [6–8]. However, the conductivity of such membranes decreases during prolonged operation because of acid leaching and other destructive processes, limiting their commercial use [9–11]. In addition to these PCM, membranes combining the characteristics of different groups are being created and studied to create highly efficient PCM that meet reliability requirements at a relatively low cost.

In this study, doped proton-conducting membranes were produced using a method based on [12]. These membranes contain phosphoric acid due to both weak hydrogen bonds with the polymer's functional groups and electrostatic interactions. The process involves creating a PPM N-phenyl-substituted polyhexamethylene guanidine/polybenzimidazole mixture, which results in the polyguanidine transforming into a polycationic form upon doping. As the content of polyguanidine in the PPM increases, the proton conductivity of the membrane sharply increases.

This study focuses on creating new doped proton-conducting membranes using a polymer-polymeric mixture of polyguanidines with a heat-resistant aromatic heterochain polymer.

Experimental

Classic methods of organic synthesis, isolation, and purification of reaction products have been used in this study. A complex of physicochemical methods of analysis (IR and NMR spectroscopy, elemental, thermogravimetric analysis, differential scanning calorimetry, microscopy) was used to characterize the obtained compounds. Studies of IR ATR spectroscopy were performed on ALPHA (Bruker, Germany), ATR attachment (ZnSe crystal), 4000–600 cm⁻¹, resolution 4 cm⁻¹. Studies of thermal decomposition of samples were performed on a NETZSCH STA 449 C synchronization thermal analyzer using air as a purge gas. The sam-

ples were recorded in the 25 ÷ 1000 °C temperature range at a heating rate of 5 °C/min. Proton conductivity was determined by the van der Pauw 4-probe method (the film of a square of 10×10 mm, at 500 Hz frequency, the amplitude voltage of 6 mV) [12] and impedance spectroscopy. The measurements were carried out by impedance spectroscopy using a Z-3000 impedance meter from Elins (Russia) in the frequency range 1 Hz–3 MHz. The amplitude of the measuring signal is 10–100 mV. Mechanical properties of the obtained film materials were tested using an Instron-3367 electromechanical rupture machine. TG, IR and mechanical properties were obtained using the equipment of the Collective Use Center of Buryat Scientific Center, Siberian branch, Russian Academy of Sciences.

The polymer-polymer mixture was prepared by mixing a 10 % solution of PHMGP in DMF and a 10 % solution of PBI in DMF at the ratios shown in the Table 1.

T a b l e   1

Ratio of polymer-polymer mixture of 10% solution of PHMGP and 10% solution of polybenzimidazole

№	PHMGP content, %	V (PHMGP10 %), ml	V(PBI, 10 %), ml
1	5.0	0.10	1.90
2	7.5	0.15	1.85
3	10.0	0.20	1.80

As the polyguanidine content increases, PPM-based film materials become brittle.

Film Doping

The dopant used was orthophosphoric acid at a concentration of 60%. The doping process involved placing a pre-weighed film into the acid solution, followed by transferring it to filter paper, removing any excess acid, and air-drying it for 24 hours at room temperature until a constant weight was achieved. The average thickness of the PCM was found to be 55±10 μm. The mass fraction of the dopant in the membrane composition of PCM (ω_{dop}) was determined using the following formula:

$$\omega_{dop} = \frac{m_{PCM} - m_{film}}{m_{PCM}} \cdot 100\ \% \ .$$

where m_{PCM} — the mass of the PCM; m_{film} — the mass of film material before doping.

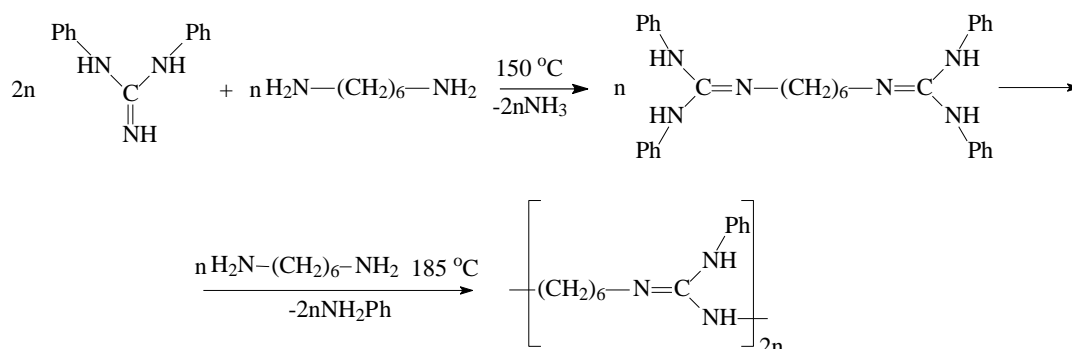Data on the composition of PCM based on PPM PHMGP/PBI are summarized in Table 2.

T a b l e   2

Composition of PCM

№	PHMGP content in PPM, %	Mass fraction of dopant, %
1	0.0	50
2	5.0	52
3	7.5	54
4	10.0	58

Results and Discussion

The synthesis of PHMGP was performed using a two-stage process with equimolar ratios of monomers, as described in reference [13], according to the scheme:

Polybenzimidazole was synthesized previously by reacting hydroxamic acid with isocyanate, as described in reference [14].

PHMGP and PBI can form single-phase stable solutions in DMF, similar to phenylone, allowing for the production of PCMs using the same method. However, increasing the content of PHMGP to more than 10% resulted in a significant deterioration of the physical and mechanical properties of the film materials, making it impossible to create PCMs based on them due to the average molecular weight of the obtained PBI. Therefore, the content of polyguanidine in PPM with PBI was limited to 10 %.
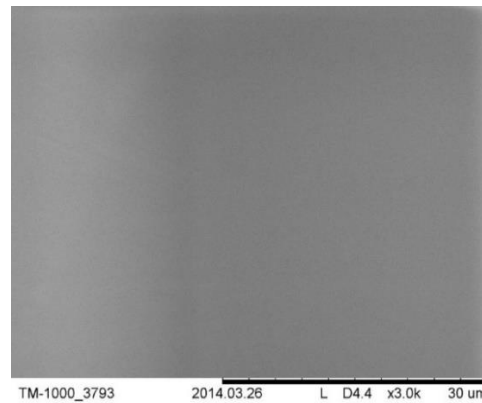

Figure 1. Micrograph of the film surface based on PPM PBI/PHMGP

On the micrograph of the film based on PBI/PHMGP PPM (Figure 1), it can be seen that there are no defects or associates, indicating satisfactory thermodynamic compatibility between the components of PPM.

Doping films containing 5 %, 7.5 %, and 10 % wt. of polyguanidine (Table 3) with similar doping levels led to an increase in conductivity, as determined by the 4-probe van der Pauw method [15, 16], indicating the influence of the polycation content.

T a b l e   3

PCM conductivity based on PBI/PGMGP

PHMGP content, wt %	σ, mS/cm after doping
–	2.8
5.0	3.1
7.5	3.4
10.0	3.8

Despite the lower content of PHMGP, the membrane's conductivity, as determined by the van der Pauw method, was $3.8 \cdot 10^{-3}$ mS/cm, which is comparable to samples obtained from PPM with phenylon with a high content of polyguanidine [12]. This behavior is likely due to partially positive and negative charges in the elementary link of PBI, which are free vacancies targeted by ions resulting from orthophosphoric acid dissociation [17]. Therefore, phenylon should be considered an "inert matrix" that does not contribute to PCM conductivity, unlike PBI. Comparing the conductivity of PCMs doped with PBI and PBI/PHMGP at room temperature and the same dopant content revealed that PPM-based membranes had a specific volumetric conductivity more than 1.5 times higher ($1.69 \cdot 10^{-3}$ and $2.82 \cdot 10^{-3}$ mS/cm, respectively), indicating a significant contribution of polyguanidine to PCM conductivity. Macromolecules of polycation are likely evenly distributed, forming a zone with high concentrations of hydrophilic components (H_2O and dissociated H_3PO_4), characterized by low resistivity. The interaction between the mixture's components is similar to that of the above-described system based on aromatic polyamide (APA):
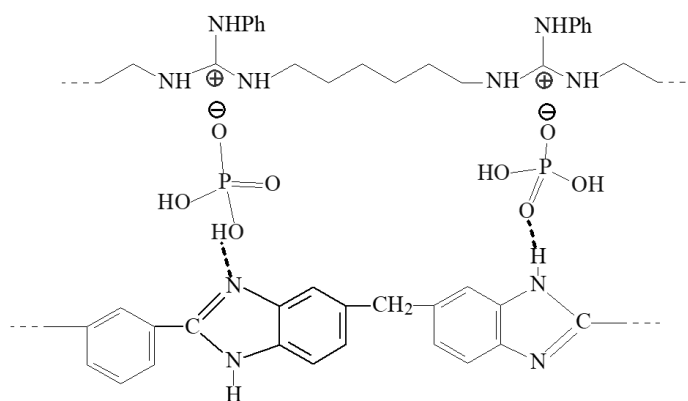
TG/DSC analysis of the doped PBI (Figure 2) and PBI/PGMGP-based PPM (Figure 3) samples shows a rather similar decomposition pattern.
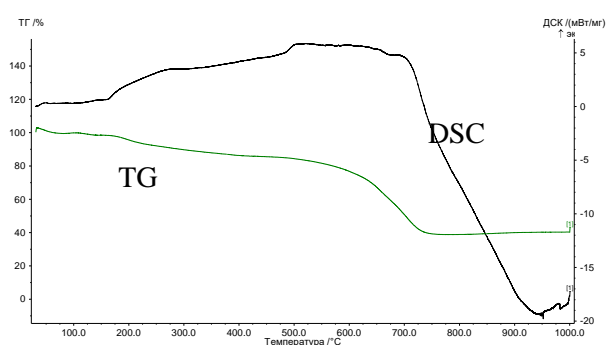

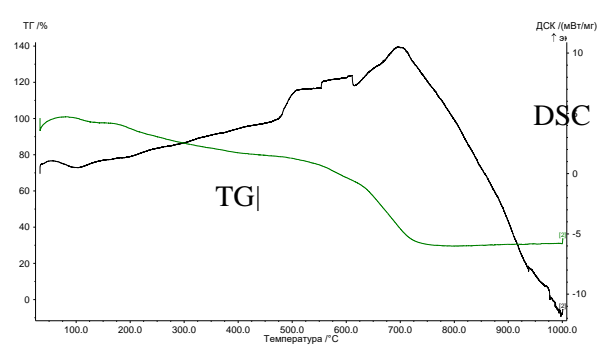Figure 2 TG/DSC curves of PBI doped

Figure 3 TG/DSC curves of the doped PPM PBI/PHMGP 10 % mass sample

There is no well-defined stepwise mass loss in the TG curves over a wide range up to 450 °C. This is due to the high resistance of PBI to thermal and thermo-oxidative destruction even in aggressive environments. Heating up to 700 °C leads to mass loss of both samples up to 35-40% and is accompanied by pronounced exothermic effects. For the doped PBI sample it is a one-step process, whereas for PBI/PGMGP two steps and a more complex pattern on DSC can be distinguished. The first step can be conventionally designated in the range of 450–600 °C and the second step — one 600–700 °C. This can be attributed to the presence of another polymer. The combination of exothermic effects and abrupt mass loss suggests intensive thermo-oxidative oxidation processes of the organic components of these systems. However, the low-temperature region is of most interest for study because it partly mimics the membrane operation in fuel cell. For the PBI/PGMGP sample (Fig. 3), an endothermic effect is observed with a peak at ~100 °C and accompanied by mass loss in the range of 100–150 °C. This is due to the partial loss of bound water. For the PBI sample (Fig. 2), this effect is practically not observed. This may be due to the presence of more hygroscopic PGMGF in the composition of the system in Fig. 3, and leads to more intense sorption of moisture from the atmosphere by the membrane surface due to its easy detachment (desorption) even at low temperature. In the temperature range of ~185–250 °C for both samples, the TG curves show a step of mass loss up to 90–85 % and its subsequent smooth decrease up to 80–75 % when reaching 450 °C. However, there are differences in the DSC curves. For PBI sample in the range 190-300 °C there is a prolonged endothermic effect. Similar behavior was not observed for the second system. It is associated with oxidative reactions starting to occur perhaps for PBI sample. For the PBI/PGMGP sample (Figure 3) the absence of a similar region on DSC presumably be explained by competing endothermic processes, such us desorption of bound water. In addition, the presence of PGMHP in its composition can lead to a marked change in the behavior of these systems with respect to sorption-desorption. The analysis of the obtained data allows us to assume that these systems (investigated PBI/PGMGP system) demonstrate high thermal stability in oxidizing atmosphere at typical temperatures of fuel cell operation in spite of the fact that some questions of thermal stability of such membranes remain not completely solved.

The sample with the maximum content of PHMGP (10% by weight) is the most interesting among the obtained membranes, therefore, other PCM-based PPMs are not further considered.

Based on PPM PHMGP/PBI, the temperature dependence of PCM was examined (Figure 4).
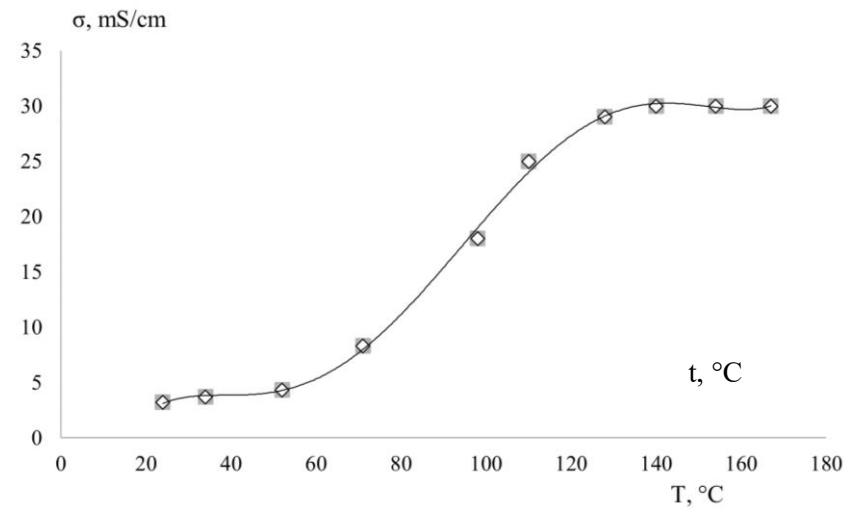

Figure 4 Temperature dependence of the specific conductivity of PCM
based on PPM PHMGP/PBI (4-probe van der Pauw method)

The behavior indicator of conductivity of membrane differs in the low and high-temperature areas. At low temperatures, the membrane's conductivity gradually increases from 3.2 mS/cm at room temperature and humidity to 8.3 mS/cm at 70 °C. In the future, due to the loss of free water by the film and subsequent temperature increase, the dependence becomes more pronounced, which is associated with the increased contribution of the Grootgus mechanism [18, 19] to the membrane's conductivity, similar to the dependence for PCM based on PPM polyguanidine with phenylone [12]. However, the membrane's further behavior is significantly different; from a temperature of 130 °C, the dependence reaches a plateau. At first glance, it may seem that the contribution of temperature increase is leveled by the destruction of the membrane; however, a detailed study of the IR spectra of the membrane before and after measurements (Figure 5), as well as the preservation of the original color and elasticity of the film, indicates the absence of destructive changes.
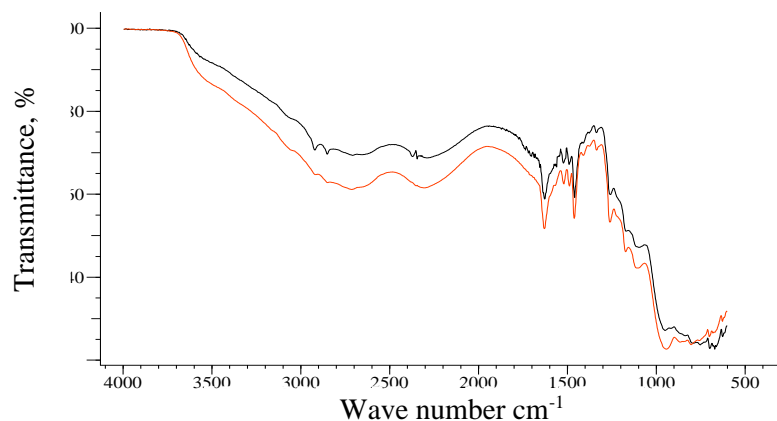

Figure 5. IR spectrum of the membrane based on PPM PHMGP/PBI
before and after measuring the temperature dependence of the conductivity

In the IR spectra, a wide absorption region in the range of 3700–2500 cm^{-1} is characteristic of strong hydrogen bonds, which partly mask the strong (intense) bands of asymmetric and symmetric oscillations of the CH$_2$ groups at 2920 and 2850 cm^{-1}, respectively. Peaks at 2700 cm^{-1} and 2330 cm^{-1} refer to the oscillations of the hydroxyl group of the dihydrogen phosphate anion. Their origin may be caused by the Fermi resonance ν(OH)-2δ(OH) [12]. The band at 1630 cm^{-1} was indicated as a characteristic peak of guanidine salts. The group of bands at 1550–1400 cm^{-1} obviously refers to oscillations of the imidazole ring of PBI. Also,

characteristic signals of oscillations of the benzene ring are in this region at 1450 cm^{-1}. This oscillation is overlapped by deformation oscillations of CH$_2$, therefore, in this case, it is not possible to reliably identify the signals of cyclic fragments related to a specific compound in the composition of PPM seems possible. The peaks in the region of 1240-1180 cm^{-1} are attributed to the P=O oscillations. Absorptions in the region of 1100–970 cm^{-1} belong to orthophosphoric acid anions [20]. Signals in the region of 900–710 cm^{-1} are characteristic of non-planar deformation oscillations of hydrogen atoms in the benzene ring (mono-substituted for PGMHP, 1,3- and 1,2,4- for PBI), however, as in the case of pulsation oscillations of the ring it is impossible to correlate them reliably for this system. Analysis of the IR spectrum of the PPM confirms the presence of the declared structural fragments according to the scheme given above. The presence of water can also lead to increased signals in the regions of 3000–3600 cm^{-1}, 2100 cm^{-1}, near 1640 cm^{-1} and below 800 cm^{-1}.

Several reasons may explain this behavior. The membrane's resistance consists of the resistance caused by the potential barrier during the migration of the proton from one acid residue to another (Rp) and the resistance of the membrane defects (Rd). If, in the first case, the resistance decreases significantly with increasing temperature, then in the second case, it does not depend on temperature. In the region of low temperatures, Rp and Rd decrease; however, with an increase in temperature, Rp decreases, and in the high-temperature region, Rd begins to prevail, and the membrane's conductivity ceases to change significantly.

Physical and mechanical tests of the obtained film materials at break — ultimate strength (σ_p) and relative elongation (ε_p) were carried out (Table 4).

Table 4

Physical and mechanical properties of film materials and PCM based on them

№	Sample	Mechanical properties	
		σ_p, MPa	ε_p, %
1	PBI nondop.	75–93	4–7
2	PBI dop.	65–80	10–14
3	PBI/PHMGP nondop.	41–46	3–6
4	PBI/PHMGP dop.	21–27	7–11

It has been shown that the addition of polyguanidine worsens the mechanical performance of the samples; however, the resulting membranes meet the requirements for PCMs [21, 22].

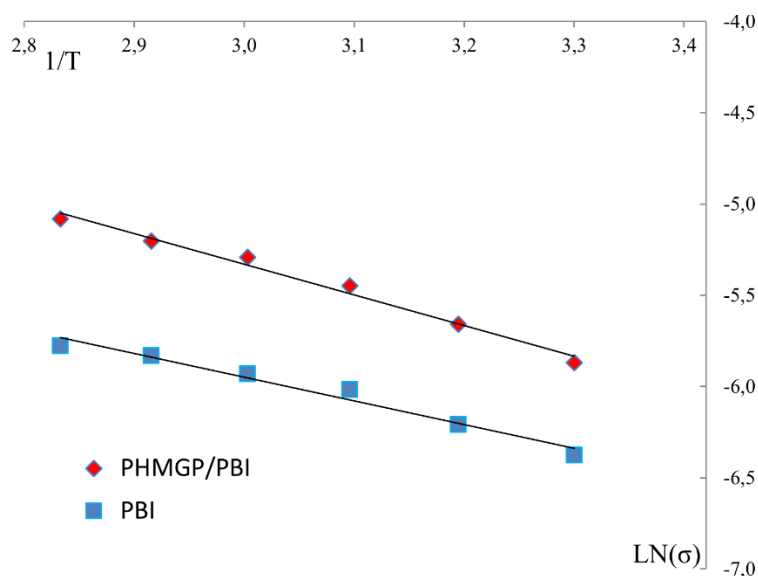In addition, such membranes are characterized by low E_a values (Figure 6, Table 5).

Figure 6. The dependence of conductivity on temperature (up to 80 ºC). Composition of PBI/PHMGP film

T a b l e 5

E_a for PCM based on PBI and PPM PHMGP/PBI

Sample	tg angle	Activation energy (E_a) eV	E_a kJ/mol
PBI	1.299	0.1123635	10.84308
PHMGP/PBI	1,675	0.1448875	13.98164

Conclusions

Using the previously developed approach to the creation of PCM [12], membranes with improved characteristics based on PPM PHMGP/PBI were obtained. The maximum specific conductivity of such membranes reaches 2.82^{10-3} mS/cm at room temperature and 0.3^{10-1} mS/cm at 130-170 °C, and 20 % weight loss is observed at a temperature of ~350°C. In addition, the membranes are characterized by satisfactory mechanical performance (σ_p = 21–27 MPa, εp = 7–11 %) and low activation energy (E_a = 0.145 eV).

Thus, the combination of good performance in the temperature range of SPEFC, good temperature resistance, satisfactory physical and mechanical characteristics, and relatively low cost of the obtained membranes allows us to consider them as promising materials for creating SPEFC.

Acknowledgments

References

1   Jiang, S., Sun, H., Wang, H., Ladewig, B.P., & Yao, Z. (2021). A comprehensive review on the synthesis and applications of ion exchange membranes. *Chemosphere*, 282:130817. https://doi.org/10.1016/j.chemosphere.2021.130817

2   Tellez-Cruz, M.M., Escorihuela, J., Solorza-Feria, O., & Compañ, V. (2021). Proton Exchange Membrane Fuel Cells (PEMFCs): Advances and Challenges. *Polymers (Basel),* 10, 13(18), 3064. https://www.doi.org/10.3390/polym13183064

3   Qu, E., Hao, X., Xiao, M., Han, D., Huang, S., Huang, Z., & et al. (2022). Proton exchange membranes for high temperature proton exchange membrane fuel cells: Challenges and perspectives. *Journal of Power Sources*, 533, 231386. https://doi.org/10.1016/j.jpowsour.2022.231386

4   Liu, H., Chen, J., Ouyang, Q., & Su, H. (2016). A Review on Prognostics of Proton Exchange Membrane Fuel Cells. 2016 IEEE Vehicle Power and Propulsion Conference (VPPC), 1-6.

5   Tang, H., Aili, D., Geng, K., Gao, J., Li, Q., & Li, N. (2021). On the stability of imidazolium and benzimidazolium salts in phosphoric acid based fuel cell electrolytes. *Journal of Power Sources*, 515, 230642. https://doi.org/10.1016/j.jpowsour.2021.230642

6   Peng, J., Fu, X., Liu, D., Luo, J., Wang, L., & Peng, X. (2022). An Effective Strategy to Enhance Dimensional-Mechanical Stability of Phosphoric Acid Doped Polybenzimidazole Membranes by Introducing in Situ Grown Covalent Organic Frameworks. *Journal of Membrane Science*, 655, 120603. https://doi.org/10.2139/ssrn.4046609

7   Yu, S., Xiao, L., & Benicewicz, B.C. (2008). Durability Studies of PBI-based High Temperature PEMFCs. *Fuel Cells,* 8, 165–174. https://doi.org/10.1002/fuce.200800024

8   Hjuler, H.A., Azizi, K., Šešelj, N., Martinez Alfaro, S., Garcia, H.R., Gromadskyi, D.G., Hromadska, L., Primdahl, S., Jensen, J.O., Li, Q., Celenk, S., & Cleemann, L.N. (2021). Durability Studies on PBI Based High Temperature PEMFC. *ECS Transactions,* 104, 403. https://doi.org/10.1149/10408.0403ecst

9   Ahmad, S., Nawaz, T., Ali, A., Orhan, M.F., Samreen, A., & Kannan, A.N. (2022). An overview of proton exchange membranes for fuel cells: Materials and manufacturing. *International Journal of Hydrogen Energy,* 47, 44, 19086-19131. https://doi.org/10.1016/j.ijhydene.2022.04.099

10 Azizi, K., Hjuler, H., Seselj, N., Jensen, J. O., Li, Q., & Cleemann, L. N. (2022). PBI-Membrane for High-Temperature PEMFC. ECS Meeting Abstracts, MA2022-02(40), 1496–1496. https://doi.org/10.1149/ma2022-02401496mtgabs

11 Park, H., Kim, H., Kim, D.-K., Lee, W. J., Choi, I., Kim, H.-J., & et al. (2020). Performance deterioration and recovery in high-temperature polymer electrolyte membrane fuel cells: Effects of deliquescence of phosphoric acid. *International Journal of Hydrogen Energy,* 45(57), 32844–32855. https://doi.org/10.1016/j.ijhydene.2020.03.039

12 Stelmakh, S. A., Ukshe, A. E., Mognonov, D. M., Novikova, K. S., Grigor'eva, M. N., Kayumov, R. R., & et al. (2016). Proton conductivity of new type medium-temperature proton exchange membranes. *Ionics*, 22(10), 1873–1880. https://doi.org/10.1007/s11581-016-1722-1

13 Bazaron, L. U., & Stel'makh, S. A. (2008). Molecular-weight characteristics of polyhexamethyleneguanidine hydrochloride. *Russian Journal of Applied Chemistry*, 81(11), 2021–2025. https://doi.org/10.1134/s1070427208110293

14 Grigor'eva, M. N., Mognonov, D. M., Tonevitskii, Yu. V., Stel'makh, S. A., & Ochirov, O. S. (2018). Aromatic Polybenzimidazoles on the Basis of 4,4′-Diphenylmethane Diisocyanate and Bis(arylene)hydroxamic Acids. *Polymer Science, Series B*, 60(1), 16–19. https://doi.org/10.1134/s1560090418010050

15 Bissessur, R., White, W., & Dahn, D.C. (2006). Electrical characterization of conductive polymers and their intercalated nanocomposites with molybdenum disulfide. *Materials Letters*, 60(2), 248–251. https://doi.org/10.1016/j.matlet.2005.08.026

16 van der PAUW, L. J. (1991). A method of measuring specific resistivity and hall effect of discs of arbitrary shape. *Semiconductor Devices: Pioneering Papers*, 174–182. https://doi.org/10.1142/9789814503464_0017

17 Zuo, Z., Fu, Y., & Manthiram, A. (2012). Novel Blend Membranes Based on Acid-Base Interactions for Fuel Cells. Polymers, 4(4), 1627–1644. https://doi.org/10.3390/polym4041627

18 Vilčiauskas, L., Tuckerman, M. E., Bester, G., Paddison, S. J., & Kreuer, K.-D. (2012). The mechanism of proton conduction in phosphoric acid. Nature Chemistry, 4(6), 461–466. https://doi.org/10.1038/nchem.1329

19 Li, Q. (2004). Water uptake and acid doping of polybenzimidazoles as electrolyte membranes for fuel cells. Solid State Ionics, 168(1–2), 177–185. https://doi.org/10.1016/j.ssi.2004.02.013

20 Goto, T., Nakanishi, K., & Ohashi, M. (1957). An Account on the Infrared Absorption of Guanidiniums. *Bulletin of the Chemical Society of Japan*, 30, 723-725.

21 Aricò, A.S., Srinivasan, S., & Antonucci, V. (2001). DMFCs: From Fundamental Aspects to Technology Development. *Fuel Cells*, 1(2), 133–161. https://doi.org/10.1002/1615-6854(200107)1:2<133::aid-fuce133>3.0.co;2-5

22 Kalhammer, F.R. (1998). Status and prospects of fuel cells as automobile engines. A Report of the Fuel Cell Technical Advisory Panel. Retrieved from https://ininet.org/fcta-p-fuel-cell-technical-advisory-panel.html

Information about authors*

Grigor'eva, Mariya Nikolaevna — Candidate of Sciences in Pharmacy, Lead Engineer of the Polymer Chemistry Laboratory, Baikal Institute of Nature Management of the Siberian Branch of the Russian Academy of Sciences (Ulan-Ude, Russia), Sakhyanova street, 6, 670047, Ulan-Ude, Russia; e-mail: Gmn_07@bk.ru; https://orcid.org/0000-0003-4184-2805

Stelmakh, Sergey Alexandrovich (*corresponding author*) — Candidate of Sciences in Chemistry, senior researcher of the Polymer Chemistry Laboratory, Baikal Institute of Nature Management of the Siberian Branch of the Russian Academy of Sciences (Ulan-Ude, Russia), Sakhyanova street, 6, 670047, Ulan-Ude, Russia; e-mail: s_stelmakh@bk.ru; https://orcid.org/0000-0003-3392-5600

_____

*The author's name is presented in the order: *Last Name, First and Middle Names*